Published OnlineFirst December 9, 2014; DOI: 10.1158/1535-7163.MCT-14-0399

Large Molecule Therapeutics

Molecular Cancer Therapeutics

ANG4043, a Novel Brain-Penetrant Peptide–mAb Conjugate, Is Efficacious against HER2-Positive Intracranial Tumors in Mice

Anthony Regina[1], Michel Demeule[1], Sasmita Tripathy[1], Simon Lord-Dufour[1], Jean-Christophe Currie[1], Mustapha Iddir[2], Borhane Annabi[2], Jean-Paul Castaigne[1], and Jean E. Lachowicz[1]

Abstract

Anti-HER2 monoclonal antibodies (mAb) have been shown to reduce tumor size and increase survival in patients with breast cancer, but they are ineffective against brain metastases due to poor brain penetration. In previous studies, we identified a peptide, known as Angiopep-2 (An2), which crosses the blood–brain barrier (BBB) efficiently via receptor-mediated transcytosis, and, when conjugated, endows small molecules and peptides with this property. Extending this strategy to higher molecular weight biologics, we now demonstrate that a conjugate between An2 and an anti-HER2 mAb results in a new chemical entity, ANG4043, which retains *in vitro* binding affinity for the HER2 receptor and antiproliferative potency against HER2-positive BT-474 breast ductal carcinoma cells. Unlike the native mAb, ANG4043 binds LRP1 clusters and is taken up by LRP1-expressing cells. Measuring brain exposure after intracarotid delivery, we demonstrate that the new An2–mAb conjugate penetrates the BBB with a rate of brain entry (K_{in}) of 1.6×10^{-3} mL/g/s. Finally, in mice with intracranially implanted BT-474 xenografts, systemically administered ANG4043 increases survival. Overall, this study demonstrates that the incorporation of An2 to the anti-HER2 mAb confers properties of increased uptake in brain endothelial cells as well as BBB permeability. These characteristics of ANG4043 result in higher exposure levels in BT-474 brain tumors and prolonged survival following systemic treatment. Moreover, the data further validate the An2–drug conjugation strategy as a way to create brain-penetrant biologics for neuro-oncology and other CNS indications. *Mol Cancer Ther; 14(1); 129–40. ©2014 AACR.*

Introduction

Breast cancer is the most common malignancy in women worldwide, accounting for more than 25% of new cancer cases reported and 14% of cancer deaths (1). Genotypic analysis of individual breast tumors led to the discovery that 25% of breast tumors and 60% of intraductal tumors overexpress the gene encoding the human epidermal growth factor receptor2 (HER2, Neu, ErbB-2, CD340); these tumors are associated with poor prognosis and a higher rate of metastasis (2, 3). The development of trastuzumab (Herceptin, Genentech), a monoclonal antibody (mAb) targeting the extracellular domain of HER2, has dramatically improved survival in patients with HER2-positive breast cancer (4, 5). Routinely administered in combination with a cytotoxic chemotherapeutic agent, trastuzumab has successfully reduced primary and metastatic HER2-positive tumors, with the exception of brain metastases. In fact, a higher incidence of brain metastases in HER2-positive breast cancer patients treated with trastuzumab has been observed (6). The observation that the majority of patients with HER2-positive tumors die of brain metastases has led to the theory that under treatment with a regimen that includes trastuzumab, migrating HER2-positive cells find the brain to be a "sanctuary site" (7). A potential explanation for trastuzumab's lack of efficacy in brain metastases is that HER2-positive status is not retained when cancer cells migrate to brain; however, a concordance between primary tumor genotype and CNS metastasic tumor genotype has been reported (8).

Further studies have established that the difficulty in treating brain metastases from HER2-positive brain tumors reflects a failure of trastuzumab to attain therapeutic exposure levels in the brain, primarily as a result of the obstacle imposed by the blood–brain barrier (BBB). Comprised of brain capillary endothelial cells with tight junctions, unfenestrated cells, and efflux pumps, the BBB limits the entry of most small-molecule and biologic therapeutics into the brain parenchyma from the circulation, preventing them from achieving therapeutic concentrations. Poor brain penetration appears to be a common feature of many mAbs (9). Even bevacizumab (Avastin, Genentech), approved in the United States for treatment of primary brain tumors, achieves only minimal exposure levels in the brain when dosed systemically (10). The efficacy of bevacizumab has been shown to result from antiangiogenic activity in the vasculature rather than brain parenchyma (11).

[1]Angiochem Inc., Montréal, Québec, Canada. [2]Département de Chimie, Université du Québec à Montréal, Montréal, Québec, Canada.

Note: Supplementary data for this article are available at Molecular Cancer Therapeutics Online (http://mct.aacrjournals.org/).

Current address for S. Tripathy: Institute for Research in Immunology and Cancer, Montréal, Québec, Canada

Corresponding Author: Jean E. Lachowicz, Angiochem Inc., 201 President Kennedy Ave, Suite 2880, Montréal, QC, Canada H2×3Y7. Phone: 514-788-7800; Fax: 514-788-7801; E-mail: jlachowicz@angiochem.com

doi: 10.1158/1535-7163.MCT-14-0399

Published OnlineFirst December 9, 2014; DOI: 10.1158/1535-7163.MCT-14-0399

A variety of methods to increase brain levels of mAbs have been tested, including coadministration with PDE5 inhibitors, coadministration with potassium channel agonists, and disruption of the BBB with mannitol or ultrasound (12–16). Modifications that enable mAbs to utilize receptor-mediated transcytosis pathways in brain capillary endothelial cells, most recently via insulin and transferrin receptors, have also been demonstrated to increase brain permeability in animals (17–19). Our approach is distinguished by the selected BBB receptor, the low density lipoprotein-like receptor-1 (LRP1). LRP1 is a member of the LDL receptor family that is highly expressed on BBB capillary endothelial cells and has been shown to transport a variety of ligands, including lactoferrin, ApoE, and β-amyloid peptide, across brain capillary endothelial cells (20–22). We have previously described a 19-amino acid peptide, derived from the Kunitz domain of multiple LRP1 ligands, which binds LRP1 and efficiently penetrates the BBB by receptor-mediated transcytosis (23, 24). Conjugation of this peptide, known as Angiopep-2 (An2), to small-molecule antineoplastic drugs like paclitaxel, doxorubicin, and etoposide, dramatically augments their uptake through the BBB following systemic administration (25, 26). One of these new agents, ANG1005, is currently undergoing phase II clinical trials in humans as a potential agent to treat primary and secondary brain tumors and has shown encouraging activity (27–29).

Here, we extend our prior studies on small-molecule An2 conjugates by examining whether incorporation of this peptide to a mAb can increase its BBB permeability and efficacy in a murine intracranial tumor model. In light of the impact of trastuzumab on HER2-positive breast cancer outside of the brain and the urgent need for a treatment for metastatic HER2-positive brain tumors, we chose to design a brain-penetrant mAb directed against HER2.

Materials and Methods

Animals

Animals were obtained from Charles River Laboratories, Inc. (St-Constant) and allowed to acclimate for 5 days before experiments. Brain perfusion studies were performed on adult male Crl: CD-1 mice (25–30 g, 6–8 weeks old). Female athymic nude mice (Crl:Nu/Nu-*nu*BR; 20–25 g, 4–6 weeks old) were used for tumor models and were maintained in a pathogen-free environment. All animals used in these studies were handled and maintained in accordance to the Guidelines of the Canadian Council on Animal Care. Animal protocols were approved by the Institutional Animal Care and Use Committee of Université du Québec à Montréal.

Reagents

BT-474 (ATCC HTB-20; 2012), SKBR3 (ATCC HTB-30; 2011), U87-MG (ATCC HTB-14; 2013), MCF-7 (ATCC HTB-22; 2001), MEF-1 (ATCC CRL-2214; 2001), and PEA-13 (ATCC CRL-2216; 2006) cells were purchased from ATCC. Cell lines were characterized for antigenic expression, DNA profile, cytogenic analysis, and isoenzyme profile by the provider. Human brain vascular endothelial cells (HBMEC) were purchased from ScienCell Research Laboratories. HBMECs are characterized by the provider by immunofluorescent methods with antibodies to vWF/Factor VIII and CD-31 (PECAM) and by uptake of DiI-Ac-LDL. Upon receipt, cells were allowed to proliferate for 1 to 2 passages to obtain aliquots for cryopreservation. For experiments, cells from frozen aliquots were resuscitated and were subcultured for no more than 5 to 10 passages according to provider instructions. Expression status of HER2 in BT-474, SKBR3, U87-MG, and MCF-7 lines and LRP1 in HBMEC was verified by Western blot analysis and immunodetection within 6 months of conducting the experiments described herein (Supplementary Fig. S1). Anti-HER2 mAb was from Eureka Therapeutics. Cross-linked dextran and D-salt dextran desalting columns and iodination beads were from Pierce. $Na^{125}I$ was from Perkin Elmer. Cyto750-NHS-ester was from Cytodiagnostics. Receptor-associated protein (RAP) from Oxford Biomedical Research and the Coomassie Plus Protein assay reagent from Thermo Scientific. Anti-human IgG (Fc-specific)-agarose antibody beads were purchased from Sigma-Aldrich.

Iodination of proteins

Anti-HER2 mAb, ANG4043 and activated α2-macroglobulin (α2M; EMD Millipore) were radiolabeled with standard procedures using an iodo-bead kit and D-Salt Dextran desalting columns. Two iodo-beads were used for the iodination of protein. Briefly, beads were washed twice with 3 mL of PBS on a Whatman filter and resuspended in 60 μL of 20 mmol/L phosphate buffer, pH 6.6. $Na^{125}I$ (1 mCi) was added to the bead suspension for 5 minutes at room temperature. Iodination of each protein was initiated by the addition of 100 μg of protein (80–100 μL of a solution in 0.1 mol/L phosphate buffer solution), pH 6.5. After incubation for 10 minutes at room temperature, iodo-beads were removed. Supernatants were applied to a desalting column prepacked with 5 mL of cross-linked dextran to remove free iodine. [^{125}I]-proteins were eluted with 5 mL of PBS. Fractions of 0.5 mL were collected, and the radioactivity in 5 μL of each fraction was measured. Fractions corresponding to [^{125}I]-proteins were pooled and further dialyzed (cut-off 10 kDa) against Ringer/HEPES, pH 7.4. Radiolabeled proteins were measured using the Bradford assay with the anti-HER2 mAb as standard.

Conjugation of anti-HER2 with Angiopep-2

Angiopep-2 was conjugated to anti-HER2 mAb using copper-free click chemistry (Fig. 1A). A two-step procedure was employed, with "Step 1" defined as the anti-HER2 modification step in which the linker moiety is incorporated onto the mAb. To a solution of anti-HER2 mAb (**1**) (3 mg/mL) in aqueous buffer (20 mmol/L sodium phosphate) at pH 8 was added a DMSO solution of MFCO-N-hydroxysuccinimide ester (**2**) (12 equiv, 7.6 mg/mL concentration) and incubated at RT for 6 hours with occasional shaking. The modified anti-HER2 mAb (**3**) was purified from excess reagent by gel filtration with a HiPrep 26/10 desalting column (GE Healthcare) using 20 mmol/L sodium phosphate buffer as eluent. To the modified octyne derivative (**3**), a DMSO solution of $An2N_3$ (**4**) (8 equiv, 8 mg/mL) was added. The solution was vortexed, wrapped with aluminum foil, and incubated overnight at room temperature. The conjugate was purified by passage through a Protein A column using a citrate-phosphate (C/P) buffer (25 mmol/L citric acid, 50 mmol/L sodium phosphate) at pH 5 for binding and a C/P buffer (40 mmol/L citric acid, 20 mmol/L sodium phosphate) at pH 3 for elution. The pH of the eluent was immediately increased to 5 with basic sodium phosphate (0.2 mol/L) solution and then dialyzed with Spectra/Por dialysis membrane (MWCO: 50,000; Spectrum Laboratories) against C/P buffer pH 5 and filtered sterile (Millipore) to obtain the anti-HER2 mAb–Angiopep-2 conjugate (**5**) (yield: 80%, 2–3

Published OnlineFirst December 9, 2014; DOI: 10.1158/1535-7163.MCT-14-0399

mg/mL). Angiopep-2 incorporation was confirmed by matrix-assisted laser desorption/ionization—time-of-flight (MALDI-TOF), SDS-PAGE, and Western blot analysis.

Electrophoresis and Western blot analysis

Anti-HER2, ANG4043, and 15 μg of whole cell lysates were separated by precast SDS-PAGE gel (Bio-Rad) and blotted onto a polyvinylidene difluoride membrane (Millipore). After transfer, immunodetection of Angiopep-2 was performed using either a mouse or rabbit mAb raised against Angiopep-2. Immunodetection of HER2 and GAPDH was performed using an anti-HER2/ErbB2 (44E7) mAb from Cell Signaling Technology and anti-GAPDH (6C5) mAb from Advanced ImmunoChemical Inc.. Horseradish peroxidase (HRP)–conjugated antibodies (Jackson ImmunoResearch Laboratories Inc.) were used as secondary antibodies and immunoreactive material was visualized with HyGLO Chemiluminescent HRP Antibody Detection Reagent (Denville Scientific Inc.).

Binding of anti-HER2 and ANG4043 conjugate

In vitro binding of anti-HER2 and ANG4043 to HER2 was determined using Herceptin (trastuzumab) ELISA kit from Alpha Diagnostic International as described by the manufacturer. Cellular binding of anti-HER2 and ANG4043 to HER2-positive BT-474 breast cancer cells was also determined. Confluent BT-474 cells were detached from flasks with PBS-citrate nonenzymatic dissociating buffer. Cells in suspension were washed in ice-cold binding buffer (BB: HEPES 10 mmol/L, NaCl 150 mmol/L, $CaCl_2$ 2.5 mmol/L, pH: 7.3), counted, and separated into individual polypropylene tubes (10^6 cells per tube). Binding of anti-HER2 mAb and ANG4043 was performed with increasing concentrations in ice-cold BB for 30 minutes at 4°C. Cells were then washed and incubated with an anti-Human-AlexaFluor488 secondary antibody (Life Technologies) in ice-cold BB for 30 minutes at 4°C. Cells were extensively washed with ice-cold BB and analyzed by flow cytometry (10,000 gated events per condition).

Cell proliferation using [^{3}H]-thymidine incorporation assay

HER2-positive cells (BT-474 and SKBR3) and HER2-negative cells (MCF-7 and U87) were cultured in 96-well white plates (Perkin Elmer) at a density of 10,000, 6,000, 10,000, and 4,000 cells per well, respectively. First, cells were synchronized for 24 hours in serum-deprived medium. After incubation of cells with unconjugated anti-HER2 mAb or ANG4043 for 5 days, all media was aspirated and cells were pulse-labeled for 4 hours at 37°C/95%O_2/5%CO_2 with media containing 2.5 μCi/mL [methyl-^{3}H] thymidine (Perkin Elmer). Cells were washed, fixed, and dried before addition of scintillation fluid (Microscint 0, Perkin Elmer). After 24 hours, cell-associated tritium was quantified by counting on a plate reader (TopCount, Perkin Elmer). Incorporated [^{3}H] thymidine was plotted for each drug concentration.

Surface plasmon resonance assay

Both LRP1 clusters II and IV were purchased from R&D Systems and were covalently coupled to a BIAcore CM5 sensor chip via primary amine groups using the N-hydroxysuccinimide (NHS)/1-Ethyl-3-(3-dimethylaminopropyl)carbodiimide (EDC) coupling agents as described by the manufacturer. LRP1 clusters to be immobilized were diluted in 10 mmol/L sodium acetate buffer at pH 4.5, followed by standard EDC/NHS coupling chemistry. Routinely, 300 to 1,000 relative units of LRP1 clusters were immobilized onto the sensor chip surface. All experiments were performed at 25°C.

Direct binding to the covalently immobilized LRP1 clusters was performed by injecting increasing concentrations (25–3,000 nmol/L) of ANG4043 or anti-HER2 mAb diluted in HBS-P+ (HEPES 10 mmol/L, NaCl 150 mmol/L, surfactant p20 0.05%, $CaCl_2$ 5 mmol/L) buffer at a flow rate of 20 mL/min, with a contact time of 120 seconds and a dissociation time of 600 seconds. The surface plasmon resonance (SPR) profile obtained for ANG4043 was compared with that of the unconjugated anti-HER2 mAb, and ANG4043 affinity for both LRP1 clusters were evaluated using BIAevaluation software.

Cellular uptake

Inhibition of [^{125}I] activated α2M cellular uptake in MEF-1 and PEA-13 cells was evaluated as follows. Cells were seeded onto plates and incubated with 2.5 nmol/L of radiolabeled [^{125}I] α2M with or without anti-HER2 mAb (5 μmol/L). ANG4043 (5 μmol/L), unlabeled α2M (1 μmol/L), or RAP (2 μmol/L for 30 minutes at 37°C. In another experiment, uptake of [^{125}I] anti-HER2 and [^{125}I]-ANG4043 was measured in HBMEC and BT-474 cells. Cells were treated with various concentrations (50, 100, or 200 nmol/L) of radiolabeled [^{125}I]-anti-HER2 and [^{125}I]-ANG4043, alone or in combination with 1 μmol/L of RAP in Ringer/HEPES buffer for 1 hour at 37°C. In both experiments, after incubation with radiolabeled mAbs, cells were washed 3 times, lysed with 0.3 mol/L NaOH for 30 minutes with shaking, and radioactivity incorporation was analyzed using a Wizard2 2470 Automatic Gamma counter (Perkin Elmer). A Bradford assay was performed on samples for protein quantitation.

Confocal microscopy

BT-474 cells were seeded onto micro cover glasses (Electron Microscopy Sciences) in 60 mm dishes. Cells were treated with or without anti-HER2 mAb or ANG4043 for 1 hour at 1 μg/mL in complete culture media (ATCC). After incubation, cells were washed and fixed with 4% paraformaldehyde in PBS for 30 minutes at 4°C. Cells were then permeabilized and blocked with 0.3% Triton X-100/1% BSA/10% FBS in PBS for 1 hour at room temperature. For HER2/ErbB2 labeling, BT-474 cells were incubated with primary antibody (#2248, Cell Signaling Technology) for 1 hour at room temperature, washed, and incubated with anti-Mouse-Alexa594 secondary antibody (Life Technologies) for 1 hour at room temperature. Detection of anti-HER2 and ANG4043 was performed by incubating anti-Human-Alexa488 secondary antibody (Life Technologies) for 1 hour at room temperature. Nuclei were stained with Hoechst 33342 (Life Technologies) at 1μg/mL for 30 minutes at room temperature. Finally, cells were washed and mounted with Prolong Gold anti-fade reagent (Life Technologies) and stored at for least 48 hours at 4°C before confocal microscopy analysis (Nikon A1).

***In situ* brain perfusion**

Brain uptake of [^{125}I]-anti-HER2 mAb and [^{125}I]-ANG4043 was measured using a mouse *in situ* brain perfusion technique based on the protocol described by Dagenais and colleagues (30). Briefly, mice were sedated before surgery with intraperitoneal ketamine/xylazine (140/8 mg/kg). The right common carotid artery was exposed and ligated at the level of the bifurcation. The common carotid was then catheterized rostrally with polyethylene tubing (0.30 mm inner diameter × 0.70 mm outer diameter)

Published OnlineFirst December 9, 2014; DOI: 10.1158/1535-7163.MCT-14-0399

filled with saline/heparin (25 U/mL) mounted on a 26-gauge needle.

Before surgery, perfusion buffer consisting of KREBS-bicarbonate buffer with 9 mmol/L glucose was prepared, incubated at 37°C, pH 7.4, and stabilized with 95%O_2:5%CO_2. A syringe containing a 2 nmol/L solution of radiolabeled compound dissolved in perfusion buffer was placed on an infusion pump (Harvard pump PHD2000; Harvard apparatus) and connected to the catheter. Immediately before the perfusion, the heart was severed and the brain was perfused for 0 to 4 minutes at a flow rate of 2.5 mL/minute. Following administration of test mAb, the brain was briefly perfused with tracer-free solution to rinse the blood vessels for 30 seconds. At the end of the perfusion, the mice were immediately sacrificed by decapitation and brains were removed. The right hemisphere was isolated on ice and homogenized in Ringer/HEPES buffer for capillary depletion (2-minute time-point samples) and ^{125}I quantitation.

Capillary depletion

The capillary depletion method was an adaptation of the method of Triguero and colleagues (31). A solution of dextran (35%) was added to the brain homogenate to give a final concentration of 17.5%. After thorough mixing by hand, the mixture was centrifuged for 10 minutes at 5,500 × g. The resulting pellet contains mainly the capillaries, whereas the supernatant contains brain parenchymal tissue. Aliquots of homogenates, supernatants, pellets, and perfusates were collected for measurement of radioactivity. [^{125}I]-samples were counted in a Wizard 2470 Automatic Gamma Counter (Perkin-Elmer Inc). All aliquots were precipitated with trichloroacetic acid (TCA) to obtain the radiolabeled precipitated protein fractions. Results were expressed in terms of volume distribution (mL/100g) for the different brain compartments.

Tissue distribution

Brain biodistribution of anti-HER2 and ANG4043 was quantified in healthy mouse brain after intravenous (i.v.) bolus injection. Tissue distribution in mouse brain was measured in normal CD-1 mice. One hour after injection of [^{125}I]-anti-HER2 or [^{125}I]-ANG4043, 10 mg/kg mAb equivalent, blood was collected and mice were cardiac-perfused with saline (5 mL/minute, 8 minutes). Brains were dissected and weighed, and radioactivity was quantified in a gamma counter. Test mAbs in serum were quantified using a Herceptin (trastuzumab) ELISA kit (Alpha International). Data were compiled and results were expressed as concentration in tissue and tissue/serum ratio. Data are presented as the mean ± SD of three individual mice.

In vivo imaging of fluorescent Cyto750-anti-HER2 and Cyto750-ANG4043

In vivo imaging was performed using the Xtreme Near Infrared Imaging system (Bruker Optics). Both anti-HER2 and ANG4043 mAbs were labeled with the NHS-Cyto750 near infrared (NiR) probe as recommended by the manufacturer (Cytodiagnostics). Briefly, mAbs (2 mg) were incubated at room temperature with a 2-fold molar equivalent of Cyto750 and incubated overnight at 4°C on a rotating mixer. Free Cyto750 was removed using a desalting column followed by extensive dialysis. The protein concentrations of labeled molecules were determined using the Bradford assay with anti-HER2 mAb as the standard. SDS-PAGE and Western blot analysis was performed to demonstrate that NiR fluorescence was associated with antibody bands.

Semiquantitative analysis was performed using MI Software version 5.0.5.29 (Bruker BioSpin). Identical illumination settings (exposure time, f/stop, filters, field of view, and binning) were used throughout image acquisition. All images were displayed in the same scale of fluorescence intensity. Fluorescence intensities were quantified using free-form manual region of interests (ROI) of equivalent sized areas. Data are presented as the mean ± SD of three individual mice.

Treatment of BT-474 brain tumor–bearing mice

Intracerebral BT-474 tumors were initiated via stereotactic inoculation of 1×10^6 BT-474 cells unilaterally into the brains of mice. One hour before surgery, mice received a subcutaneous injection of buprenorphine (0.1 mg/kg). For tumor cell inoculation, mice were placed in a stereotactic apparatus (Kopf) and maintained under anesthesia with isoflurane. A burr hole was drilled 1.5 mm anterior and 2.5 mm lateral to bregma. Cells suspended in 5 μL of serum-free cell culture medium containing 0.5% methylcellulose were injected over a 5-minute period using a Hamilton syringe at a depth of 3.5 mm. Drug treatments began 12 days after tumor cell inoculation. After dialysis, both unconjugated anti-HER2 mAb and ANG4043 were administered in sodium acetate buffer (150 mmol/L NaCl, 5 mmol/L NaOAc, pH 5). The concentration of both mAbs was adjusted to allow a 5 to 6 mL/kg injection volume for all doses. Clinical signs of disease progression and body weights were monitored daily. When mice reached terminal endpoints (20% body weight loss, mobility impairment), they were sacrificed by carbon dioxide asphyxiation.

Statistical analysis

Data are expressed as mean ± SD or SEM. Statistical analyses were performed using student *t* tests when one group was compared with the control group. For two or more groups, ANOVA with *post hoc* Dunnett test was used. For the survival study, log rank (Mantel–Cox) test was used for statistical analysis. All statistical analyses were performed using GraphPad Prism 5 for Windows (GraphPad Software Inc.) with the exception of survival studies, where MedCalc Software (Ostend) was used. Significance was assumed for $P < 0.05$.

Results

Synthesis and *in vitro* characterization of ANG4043

Multiple peptide–mAb conjugates were produced using various linkers, conjugation reactions, and Angiopeps, leading to selection of ANG4043. This conjugate is prepared by attaching An2 to free amines present on an anti-HER2 mAb using copper-free click chemistry (Fig. 1A). Incorporation of An2 was confirmed by MALDI-TOF mass spectrometry, SDS-PAGE, and Western blot analysis using an antibody directed against An2. The change in mass from 148,041 to 159,626 Da indicates that four An2 peptides are conjugated to the mAb (Fig. 1B). SDS-PAGE under nonreducing conditions followed by Coomassie blue staining shows ANG4043 migration at a higher molecular weight than native anti-HER2, and Western blot analysis with immunodetection of the An2 peptide further confirms the presence of An2 on ANG4043 (Fig. 1C). An2 was detected on both heavy and light chains of ANG4043 when Western blot analysis was performed under reducing conditions (Supplementary Fig. S2).

HER2 binding and antiproliferative activity of ANG4043

Evaluation of HER2 binding was conducted with mAbs to determine the impact of An2 conjugation on antigen targeting

Published OnlineFirst December 9, 2014; DOI: 10.1158/1535-7163.MCT-14-0399

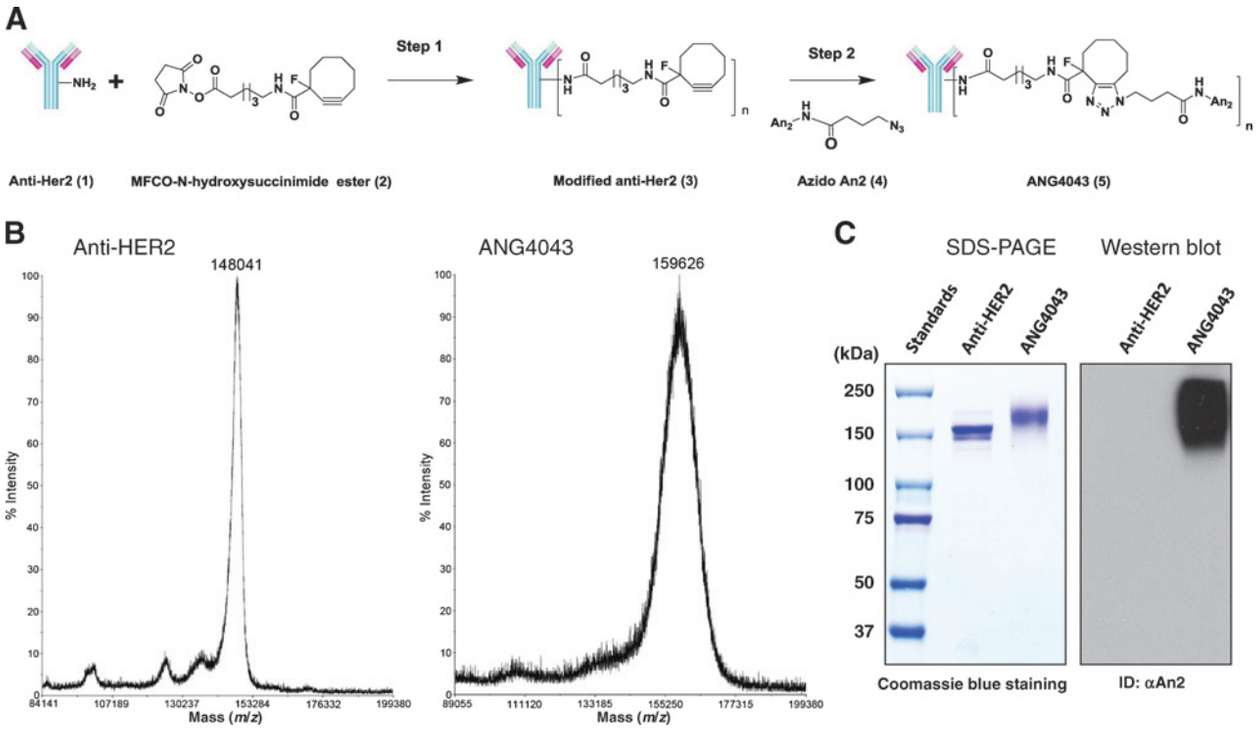

Figure 1.
Synthesis and characterization of ANG4043. A, schematic representation of the two-step synthesis of ANG4043. B, MALDI-TOF analysis of ANG4043 compared with unconjugated anti-HER2 mAb. C, characterization of anti-HER2 mAbs with SDS-PAGE and Western blot analysis with anti-An2 detection. SDS-PAGE was performed on anti-HER2 and ANG4043 under nonreducing conditions followed by staining with Coomassie blue or Western blot analysis with immunodetection of An2 to demonstrate An2 incorporation.

(Fig. 2). First, binding site localization for ANG4043 and anti-HER2 was visualized in live cells using confocal microscopy (Fig. 2A). HER2 receptors were detected on the BT-474 cell surface using a mouse anti-human HER2 primary antibody and an Alexa594 (red)-labeled anti-mouse IgG secondary antibody. After a 1-hour incubation, both mAbs were similarly detected at the cell surface of BT-474 cells using an Alexa488 (green)-labeled anti-human IgG antibody. Colocalization of this binding with red fluorescence-marked HER2 receptors (resulting in a merged yellow signal) indicates that ANG4043 targets the HER2 antigen expressed on the cell surface of tumor cells as well as the native mAb. To determine the affinity of the mAbs for HER2, cellular binding to HER2-positive BT-474 breast ductal carcinoma cells was performed and analyzed by flow cytometry. K_d values were 1.7 ± 0.2 nmol/L for ANG4043 and 1.5 ± 0.2 nmol/L for anti-HER2 control (Fig. 2B). Similar *in vitro* binding to the HER2/Fc chimera protein was observed for conjugated and native mAbs (Supplementary Fig. S3A). These results demonstrate that ANG4043 retains its affinity for the HER2 antigen, either in purified form or expressed on the surface of cancer cells.

Having confirmed the interaction between ANG4043 and HER2, we next assessed the functionality of ANG4043 by measuring its effects on cell proliferation *in vitro* using a [^{3}H] thymidine incorporation assay. Antiproliferative activity of each mAb was evaluated in HER2-positive and HER2-negative cell lines. ANG4043 and the anti-HER2 mAb exhibited equipotent inhibition of BT-474 cell proliferation with IC_{50} values of 3.7 ± 1.7 nmol/L for ANG4043 and 3.6 ± 1.6 nmol/L for the native mAb (Fig. 2C). In SKBR3 cells, which are also HER2-positive, IC_{50} values were 0.9 ± 0.7 and 0.4 ± 0.1 nmol/L for ANG4043 and anti-HER2, respectively (Fig. 2D). For both antibodies, the antiproliferative effects on BT-474 and SKBR3 appear to be due to HER2 targeting, as neither inhibited proliferation of HER2-negative MCF-7 breast adenocarcinoma cells, which have been previously shown to be insensitive to anti-HER2 effects *in vitro* (5) or U-87 glioma cells (Supplementary Figs. S3B and S3C).

LRP1 binding and cellular uptake of ANG4043

To demonstrate the interaction between ANG4043 and LRP1, a series of binding and uptake experiments were conducted. LRP1 contains four extracellular binding domains referred to as clusters I–IV; these are routinely used for affinity measurements and most LRP1 ligands are reported to bind to clusters II and IV (32). First, SPR was used to monitor the potential real-time interaction of both mAbs with these two LRP1 clusters. In this approach, LRP1 cluster II and LRP1 cluster IV were immobilized on a BIAcore CM5 sensor chip using standard amine chemistry. Increasing concentrations of ANG4043 and anti-HER2 were applied to immobilized LRP1 clusters. As shown in Fig. 3A, only ANG4043 generated a concentration-dependent increase in SPR signal when injected over LRP1 clusters. Affinity constants were estimated by plotting the SPR signal as a function of ANG4043 concentration. The K_d values obtained for cluster II and cluster IV for ANG4043 were 1.0 and 1.3 μmol/L, respectively.

To demonstrate the interaction between ANG4043 and full-length LRP1 expressed in mammalian cells, [^{125}I]-activated α2M

Published OnlineFirst December 9, 2014; DOI: 10.1158/1535-7163.MCT-14-0399

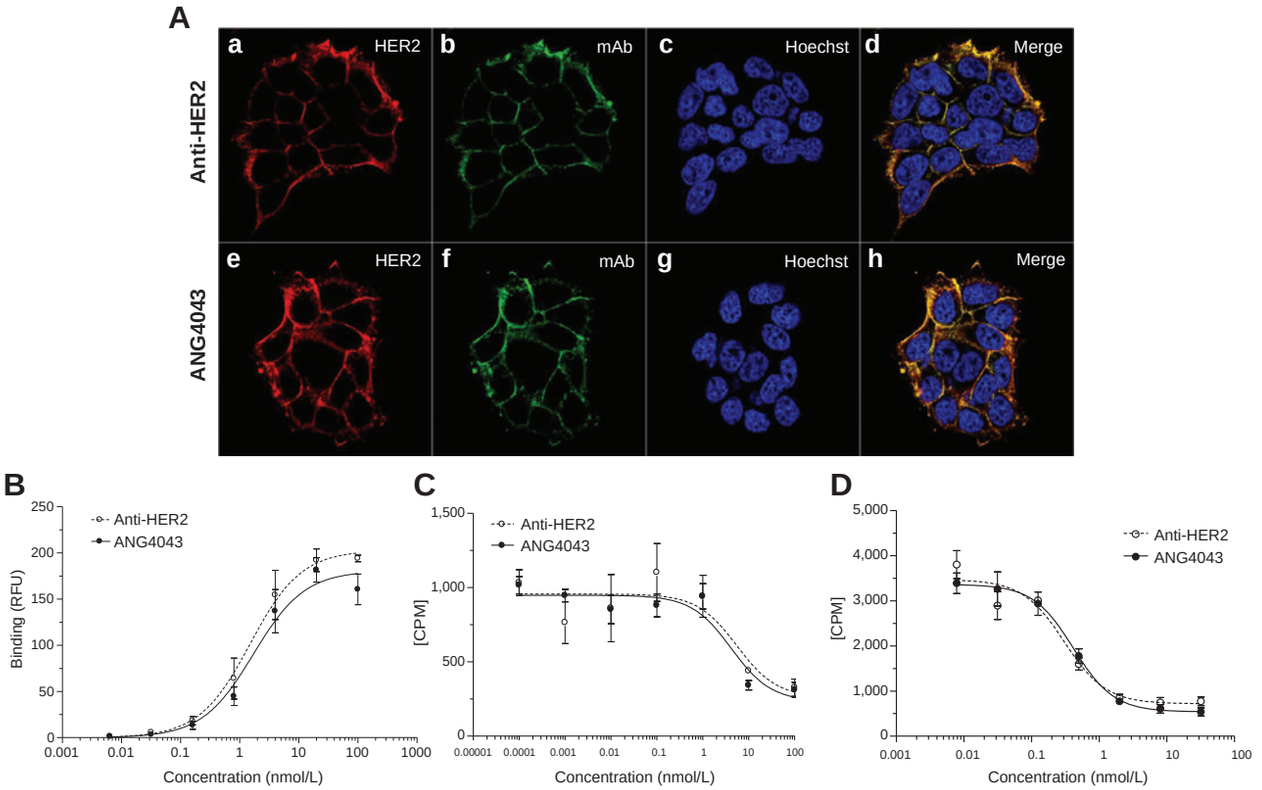

Figure 2.

Binding and antiproliferative effects of ANG4043 and anti-HER2 mAbs on tumor cells. A, confocal microscopy showing cellular localization of mAbs on BT-474 cells. After a 1-hour incubation of BT-474 cells with anti-HER2 or ANG4043 (1 μg/mL), confocal microscopy was performed to visualize localization of HER2 receptor and mAbs. Cell surface localization of HER2 receptor is shown in red (a, e) and native anti-HER2 (b) or ANG4043 (f) in green. Nuclei were Hoechst-stained blue (c, g). A merge of the three signals shows overlapping cell surface distribution between the antibodies and the HER2 receptor in yellow (d, h). Representative images from three experiments are shown. B, binding of mAbs to HER2-positive BT-474 breast cancer cells ($n = 3$ experiments performed in duplicate). C, antiproliferative effect of anti-HER2 and ANG4043 on HER2-positive BT-474 cells. D, antiproliferative effect of mAbs on HER2-positive SKBR3 cells. Antiproliferative evaluation on cancer cells was performed using [^{3}H] thymidine incorporation assays two times in quadruplicate. Data represent the mean ± SD.

binding assays were conducted using LRP1-positive MEF1 cells and LRP1-negative PEA-13 cells (Fig. 3B). In the LRP1-positive cells, [^{125}I]-α2M binding was observed and was reduced in the presence of ANG4043 (5 μmol/L) or LRP1 ligands receptor-associated protein (RAP, 2 μmol/L) and unlabeled α2M (1 μmol/L). ANG4043 also reduced radioligand binding by 60%, whereas the unconjugated anti-HER2 mAb did not compete with [^{125}I]-α2M. As expected, binding of [^{125}I]-α2M to LRP1-negative cells was much lower and unaffected by LRP1 ligands or mAbs, illustrating the specificity of ANG4043 inhibition on LRP1-positive MEF-1 cells. We next examined whether ANG4043 could be taken up by HBMEC, which express LRP1. At increasing concentrations of mAb, HBMEC uptake is significantly higher for ANG4043 than for native mAb (Fig. 3C). The LRP1 ligand, RAP (1 μmol/L), inhibits ANG4043 uptake, whereas the minor uptake of anti-HER2 is unaffected by RAP (Fig. 3D). As these endothelial cells are HER2-negative, these results demonstrate LRP1-dependent uptake of ANG4043 that is conferred by the An2 moiety.

Brain penetration of ANG4043

The cerebrovascular permeability of ANG4043 was analyzed using an established *in situ* brain perfusion assay (33). To perform this protocol, radiolabeled mAbs were administered to sedated mice via the carotid artery, thereby avoiding first pass metabolism. Saline was perfused before sacrifice to eliminate any mAb remaining in the intracranial circulation or associated with capillary endothelial cells. Quantitation of radioactivity in the brains of mice sacrificed at various time points following mAb administration was used to calculate the K_{in}, the rate constant for brain entry. Using this approach, the K_{in} for anti-HER2 was found to be 2.4×10^{-4} mL/g/s, whereas the K_{in} for ANG4043 was 1.6×10^{-3} mL/g/s (Fig. 4A). Using the same species and method, Dagenais and colleagues reported K_{in} values for a variety of compounds (34). For comparison, the K_{in} for the unconjugated anti-HER2 mAb is close to that of the antiviral drug ritonavir K_{in} (3.0×10^{-4} mL/g/s), which is classified having low CNS penetration (35). In contrast, the Kin for ANG4043 is close to that of the CNS-active anticonvulsant drug gabapentin, 2.5×10^{-3} mL/g/s.

Theoretically, association of ANG4043 with brain tissue following saline perfusion might result from the agent trapped within or affixed to the BBB capillary endothelial cells, rather than truly passing through them into brain parenchyma. To examine this issue, we used a capillary depletion protocol that separates brain capillaries from parenchymal tissue. Following this procedure, approximately 60% of the ANG4043-associated

Published OnlineFirst December 9, 2014; DOI: 10.1158/1535-7163.MCT-14-0399

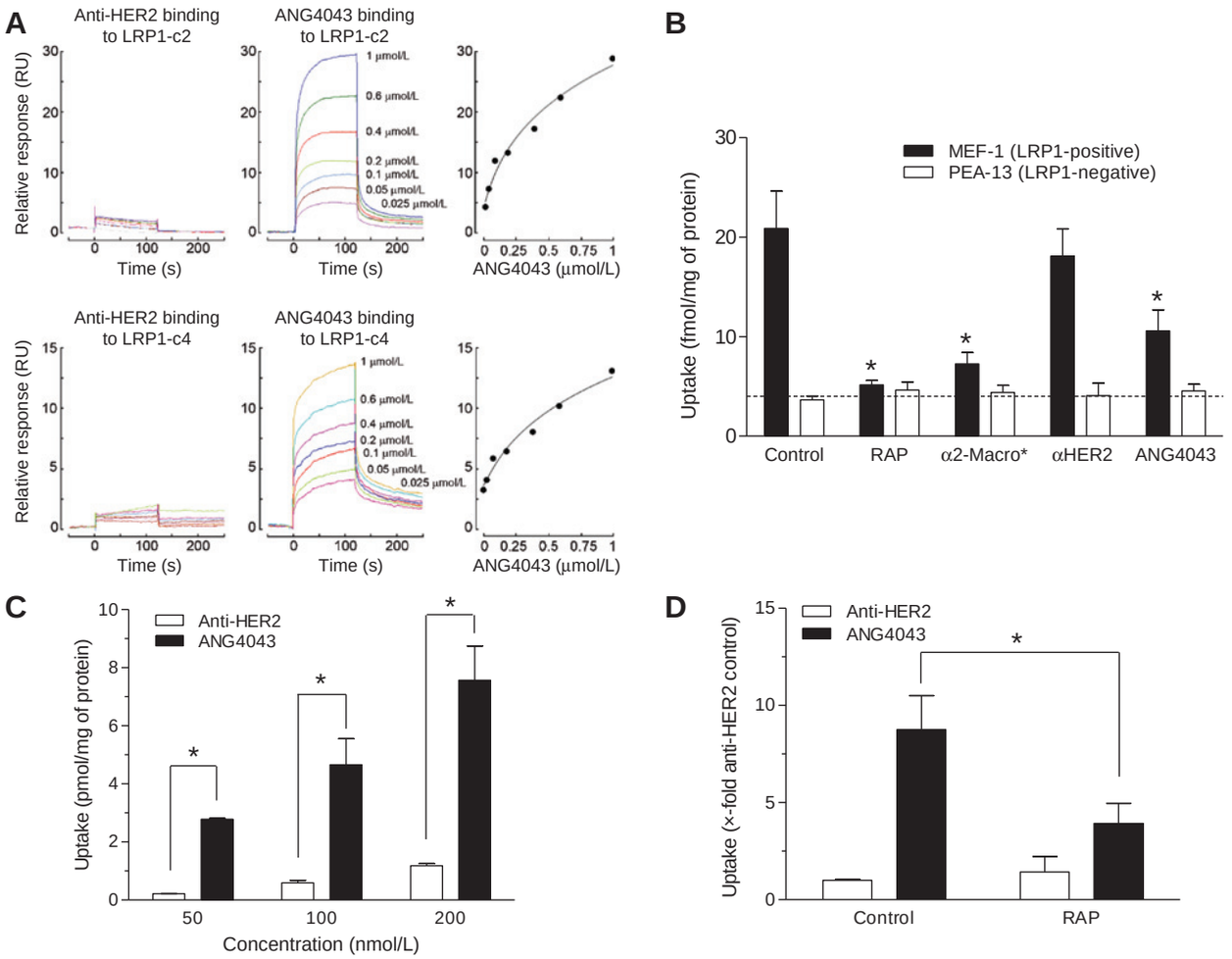

Figure 3.
Interaction with LRP1 and uptake of [^{125}I] anti-HER2 mAb derivatives in cells. A, ANG043 interaction with LRP1 cluster II and cluster IV was monitored by SPR. LRP1 clusters II and IV were immobilized on a BIAcore sensor chip and exposed to increasing concentrations of either anti-HER2 or ANG4043. SPR signal at steady state was then plotted as a function of ANG4043 concentration. From these curves, the K_d values for ANG4043 binding to LRP1 clusters II and IV were derived using BIAevaluation software. B, inhibition of [^{125}I]-α2M uptake in MEF-1 (LRP1-positive) and PEA-13 (LRP1-negative) cells. MEF-1 and PEA-13 cells were incubated with 2.5 nmol/L radiolabeled [^{125}I]-α2M for 30 minutes at 37°C in the presence or absence of receptor-associated protein (RAP; 2 μmol/L), unlabeled α2M (1 μmol/L), anti-HER2 (5 μmol/L), or ANG4043 (5 μmol/L). After incubation and washing, radioactivity associated with the MEF-1 and PEA-13 cells was quantified. Results are expressed in terms of fmol/mg of protein. C, uptake of [^{125}I]-anti-HER2 and [^{125}I]-ANG4043 in HBMEC after a 1-hour incubation. D, inhibition of [^{125}I]-ANG4043 uptake in HBMEC by RAP. HBMEC were incubated with 200 nmol/L [^{125}I]-anti-HER2 and [^{125}I]-ANG4043 with or without RAP (1 μmol/L) for 1 hour at 37°C. Uptake results are expressed in terms of fold over anti-HER2 uptake measured in control wells. Uptake data represent the mean ± SD of two experiments performed in duplicate (*, $P < 0.01$).

signal was localized to the parenchymal fraction rather than capillary fraction (Fig. 4B), thus demonstrating the ability of ANG4043 to cross the BBB. The efficiency of passage of ANG4043 into brain parenchyma exceeds than that of the native mAb by 16-fold. The potential influence of antibody–antigen interaction on brain exposure was avoided, as these studies were conducted in healthy mice which do not express the HER2 receptor target of the mAb.

Mice without tumors were also used for pharmacokinetic and brain distribution studies. Serum levels at times between 15 minutes and 30 days following i.v. administration of ANG4043 or native mAb (10 mg/kg equivalent) were measured using an ELISA (Fig. 4C). Serum concentrations of ANG4043 are lower than those of native mAb at all times measured, indicative of a higher volume of distribution for ANG4043 than anti-HER2 (11.8 vs. 7.3 mL, respectively). This result is expected, as LRP1 expression in numerous organs including liver is likely to contribute to increased distribution to those tissues as well as brain. The terminal half-life of ANG4043, 8.5 days, is similar to that of anti-HER2, 11.4 days, suggesting that a similar dose regimen would be appropriate.

Determination of the amount of ANG4043 in brain following a 10 mg/kg i.v. dose was performed using [^{125}I]-radiolabeled mAb, as the presence of brain tissue interferes with ELISA detection. One hour after administration, serum was collected and a whole body saline perfusion was conducted to eliminate circulating mAb before harvesting brains. Concentrations of ANG4043 and anti-HER2 in brain were 6.43 and 1.86 nmol/L (1.03 and 0.29

Published OnlineFirst December 9, 2014; DOI: 10.1158/1535-7163.MCT-14-0399

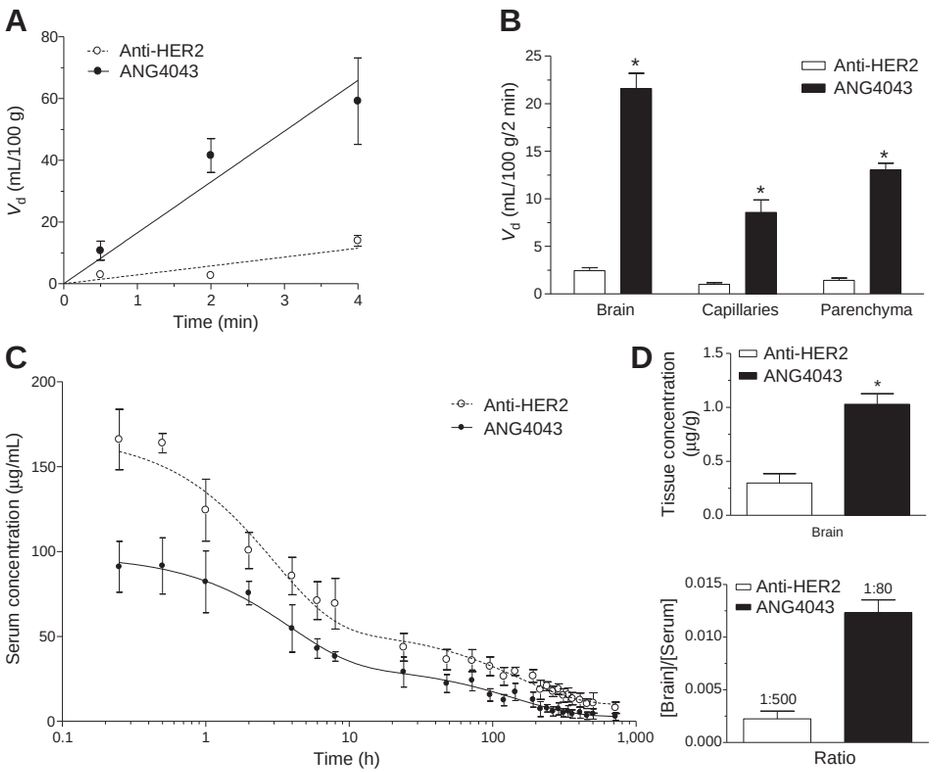

Figure 4.
Demonstration of brain penetration of ANG4043. A, volume of distribution in brain of [^{125}I]-radiolabeled ANG4043 and anti-HER2 mAbs following systemic perfusion via the carotid artery. The rate constant for brain entry, K_{in}, is derived from the slope of the line. Data represent the mean ± SEM ($n = 8$). B, volume of distribution in total brain, capillary fraction, and parenchymal fraction at the 2-minute time point. Data represent the mean ± SEM ($n = 4$; *, $P < 0.02$; two-tailed t test). C, plasma pharmacokinetics of ant-HER2-mAb and ANG4043 measured in mice. Data represent the mean ± SEM. ($n = 4$ mice per time point). D, brain concentration of radiolabed anti-HER2 and ANG4043 after i.v. bolus injection. Radiolabeled mAbs were injected at 10 mg/kg in the tail vein of mice. After 1 hour, serum was collected and whole body saline perfusion was performed. The brains were then removed and radioactivity present in the brain was quantified. Results are expressed in terms of μg/g of tissue and in terms of brain/serum ratio for mAbs ($n = 3$; *, $P < 0.02$).

μg/g), respectively. As serum levels for ANG4043 were slightly lower, these brain concentrations correspond to a brain/serum ratio of 0.012 (1:80) for ANG4043, which is 6-fold higher than the brain/serum ratio for anti-HER2, 0.002 (1:500, Fig. 4D). In a separate experiment in which mice with intracranial BT-474 cell tumors were administered 10 mg/kg ANG4043, i.v. 1 hour before sacrifice, An2 was immunodetected on both heavy and light chains of ANG4043 immunoprecipitated from brain tumor homogenates. These results indicate that the An2 peptide remains attached to ANG4043 following its entry into tumoral brain. (Supplementary Fig. S4).

In vivo accumulation of ANG043 in BT-474 brain tumors

To visualize mAbs in brains of tumor-bearing mice, BT-474 cells were implanted intracerebrally via unilateral stereotactic inoculation, and the human tumor xenografts were allowed to expand for 40 days. Following this time period, fluorescent Cyto750-labeled mAbs were administered systemically in a single intravenous bolus dose of 10 mg/kg. NiR imaging performed 24 hours later showed little accumulation of fluorescent signal in the head region of mice dosed with the native mAb, consistent with low passage through the BBB (Fig. 5A). Images taken from mice treated with Cyto750-ANG4043 showed a stronger fluorescent signal in the overall brain region than was observed with Cyto750-anti-HER2 administration. Furthermore, the highest fluorescence intensity was localized within the brain hemisphere that received intracranial BT-474 cell implantation. Corresponding fluorescence intensity measurements are shown in Fig. 5B. Following sacrifice and removal of brains from mice, large tumors were observed in this brain region, confirming that the BT-474 cells had matured into a tumor mass. In a sham study where mice were subject to stereotactic implantation of buffer without cells, systemic administration of fluorescent mAbs generated a very faint and homogenous fluorescent signal without fluorescent hot spots, indicating that the increase in fluorescent signal with Cyto750-ANG4043 was not associated with the intracranial surgery.

In vivo efficacy in mice bearing BT-474 brain tumors

If the level of BBB transport is sufficient to drive therapeutic concentrations of the mAb to the brain, ANG4043 treatment to mice with intracranial tumors would be expected to confer a survival advantage. To assess this possibility, mice were intracranially implanted with BT-474 cells and were then treated with vehicle, anti-HER2, or ANG4043 twice weekly at dose of 5 mg/kg initiated 12 days after tumor cell implantation. The twice weekly

Published OnlineFirst December 9, 2014; DOI: 10.1158/1535-7163.MCT-14-0399

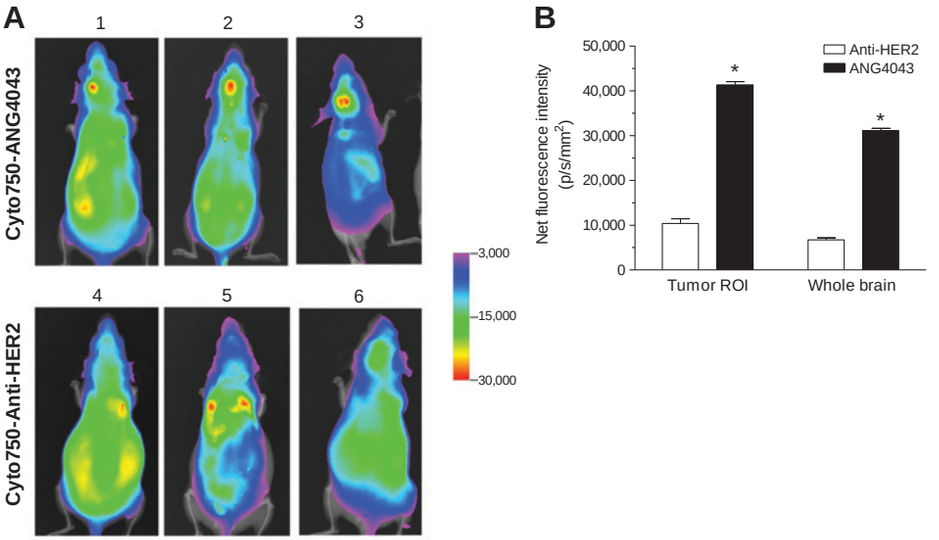

Figure 5.
NiR imaging in mice bearing BT-474 intracranial tumors. A, NiR images taken 24 hours after tail-vein injection of Cyto-750–labeled anti-HER2 or Cyto-750–labeled ANG4043 in mice that had been implanted with HER2-positive BT-474 cells 36 days earlier. Color quantitation is displayed such that violet depicts lowest intensity and red depicts highest intensity, corresponding to lowest and highest level of exposure, respectively. B, NiR fluorescence of Cyto750-anti-HER2 and Cyto750-ANG4043 was quantified for the whole brain and region of interest (ROI, tumoral hemisphere). Results are expressed in terms of net fluorescence intensity (p/s/mm^2). Data represent the mean ± SEM. ($n = 3$; *, $P < 0.02$).

regimen in this study was selected to be consistent with numerous trastuzumab mouse survival studies reported in the literature, including those evaluating effects in brain (15, 36–40). Before starting survival studies, tolerability was confirmed in separate groups of mice with doses as high as the limit of solubility; 50 mg/kg. At this dose, ANG4043 was well tolerated. Mice ($n = 10$) in the survival studies were monitored daily for body weight loss and were euthanized if a reduction of 20% or greater from the maximum weight was observed. For the native mAb, median survival was somewhat higher than for vehicle (6%, $P = 0.028$), with vehicle and anti-HER2 median survival of 47 days [95% confidence interval (CI), 40–50] and 50 days (95% CI, 45–56), respectively (Fig. 6A). A pronounced increase in survival was noted for ANG4043 compared with both the vehicle (28% increase; $P = 0.0012$) and the unconjugated mAb (20% increase; $P = 0.019$). Median survival in the ANG4043 group was 60 days (95% CI, 50–63). In a follow-up study to determine the effect of increasing dose, intravenous treatment with 15 mg/kg ANG4043 increased median survival by 78% ($P = 0.0003$), with survival of 45 days (95% CI, 40–49) in the vehicle group and 80 days (95% CI, 62–89) in the ANG4043 group (Fig. 6B). One mouse in the ANG4043 group survived well beyond the others in the cohort and was terminated on day 127 to end the study.

Discussion

Conjugation with the 19–amino acid peptide An2 has been reported to confer brain permeability to small molecules (41) and peptides (42). Interestingly, studies independent of our laboratory demonstrated that An2 can also be used in drug delivery systems such as liposomes and nanoparticles to transport a wide variety of molecules including anticancer and antifungal drugs (43–45). The current study objective was to determine whether incorporation of this peptide to mAbs would result in BBB penetration sufficient to achieve therapeutic brain concentrations. Conjugation of An2 to anti-HER2 was performed using copper-free click chemistry, producing a new chemical entity called ANG4043, which retains high HER2 receptor affinity and antiproliferative potency in HER2-positive BT-474 and SKBR3 cells. Confocal microscopy demonstrated colocalization of ANG4043 and HER2 on the BT-474 cell surface after a 1-hour incubation. Taken together, these results confirm that the pharmacologic properties of ANG4043 with respect to HER2 targeting are intact. By conjugating An2 to the anti-HER2 mAb, we have created a bifunctional molecule that interacts with LRP1 as well as HER2. In previous studies, we reported colocalization between Alexa488-An2 and LRP1 in an *in vitro* bovine brain endothelial cell BBB model (23). In the current study, we demonstrate that ANG4043 uptake by HBMEC is pronounced and is attenuated in the presence of the LRP1 ligand, RAP. At a concentration similar to that achieved in mouse brain following a single systemic dose, ANG4043 competes for [^{125}I] α2M binding in cells that express LRP1, but not in LRP1-negative cells. Finally, ANG4043 binds to LRP1 clusters II and IV with affinities of 1.0 and 1.3 μmol/L. These values are in agreement with the Km for uptake of the An2 peptide (1.2 μmol/L) from U87 cells, which express LRP1 (27). Clearly, an An2 and LRP1-dependent mechanism of uptake into endothelial cells is utilized by ANG4043 but not by unconjugated mAb. ANG4043's moderate affinity for the LRP1 receptor may be advantageous to receptor-mediated transcytosis. Yu and colleagues (18) reported that an antibody with high affinity (20 nmol/L) to transferrin receptors (TfR) remained associated with the BBB, while a lower affinity variant (600 nmol/L) was able to disassociate from the BBB and achieve higher parenchymal concentrations.

A critical objective for any new CNS therapeutic is to demonstrate entry into brain parenchyma, where the target resides. As some agents exhibit high association with brain capillary endothelial cells, assessment of total brain homogenates following

Published OnlineFirst December 9, 2014; DOI: 10.1158/1535-7163.MCT-14-0399

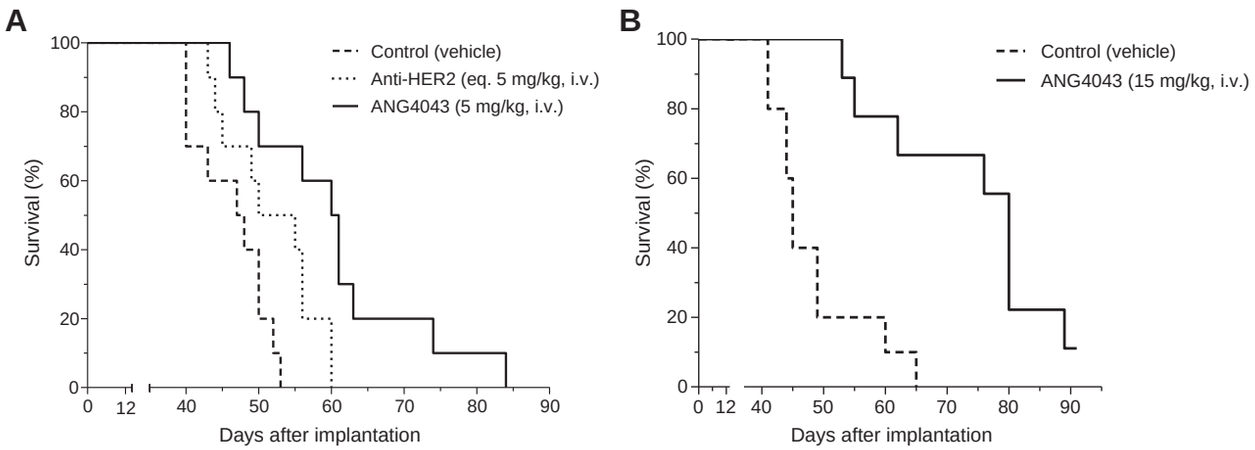

Figure 6.
Survival curves of mice with intracranial HER2-positive brain tumors. BT-474 cells were implanted into the brains of mice as described in the Materials and Methods section. Drug treatments were initiated 12 days after tumor cell implantation. A, mice were treated twice weekly with 5 mg/kg of ANG4043, 5 mg/kg equivalent of anti-HER2, or vehicle, i.v. ($n = 10$). Clinical signs of disease progression and body weight were monitored daily. Compared with the vehicle control group (47 days), survival in the anti-HER2 group was increased by 6% to 50 days [$P = 0.028$ compared with control, log-rank (Mantel–Cox) test] and in the ANG4043-treated group by 28%, to 60 days ($P = 0.0012$ compared with control; $P = 0.019$ compared with anti-HER2). B, mice were treated twice weekly with 15 mg/kg of ANG4043 or vehicle, i.v. ($n = 10$). Treatment with 15 mg/kg ANG4043 increased median survival by 78% [80 days compared with 45 days, $P = 0.0003$ for ANG4043 compared with control, log-rank (Mantel–Cox) test].

dosing is insufficient to determine whether this goal has been achieved. In the current study, multiple methods were used to confirm that ANG4043 reached the brain parenchyma, even in the absence of HER2 target expression, using healthy, non–tumor-bearing mice. First, saline perfusion was performed following all *in situ* brain perfusion experiments to clear any mAb that may have associated nonspecifically with brain capillaries. Second, a capillary depletion protocol was used to separate vessel-associated mAb from parenchymal mAb. In these experiments, significantly greater signal was associated with parenchymal fractions in mice that received ANG4043 compared with those that received anti-HER2. Finally, *in vivo* NiR imaging demonstrated a more dense localization of signal within the tumoral brain hemisphere following treatment with Cyto750-ANG4043, suggesting association of the peptide–mAb conjugate with HER2 receptors on intracranial BT-474 xenografts. In comparison, the signal associated with Cyto750-anti-HER2 was much weaker and more diffuse, suggestive of low brain permeability.

The observed increase in brain penetration of ANG4043 adds to the body of evidence supporting receptor-mediated transcytosis as a means to create brain-penetrant macromolecules. Furthermore, this work is the first demonstration of an antibody rendered brain penetrant by conjugation with a small (19 AA) peptide. Other recent advances using receptor-mediated transcytosis have been based on a strategy that requires modification of the antibody with a large protein moiety. This approach may be difficult to translate to other types of molecules, such as peptides and enzymes, without altering target binding or function. An2 has been conjugated to peptides such as the tridecapeptide neurotensin (ANG2002) without loss of receptor-binding affinity, resulting in an agent that demonstrates efficacy in rodent pain models on systemic dosing (42).

Targeting LRP1 as opposed to other receptors that mediate transcytosis, such as TfR, may also be advantageous. Prolonged *in vitro* exposure to an anti-TfR antibody was reported to cause TfR downregulation, which could affect safety and tolerability (19). In a separate study using a different TfR targeting mAb, a decrease in reticulocyte count in mouse was reported (46). In contrast, the use of An2 to target LRP1 for brain penetration has been tested in humans. An An2–paclitaxel conjugate in phase II studies for primary and secondary brain tumors, ANG1005, has been dosed to more than 200 patients, and no adverse events beyond those associated with paclitaxel have been reported (28, 29). The majority of these patients received multiple cycles of the drug, with the longest treatment duration being 87 weeks.

ANG4043 retains its pharmacologic properties after crossing the BBB, indicated by the localization of fluorescent ANG4043 to BT-474 xenografts in brain. Moreover, in a survival study, ANG4043 treatment was associated with a significantly greater improvement in survival than anti-HER2. The small increase in median survival for the native mAb is consistent with the low concentrations observed in brain, while the increased survival conferred by ANG4043 suggests that the higher brain concentrations provide additional benefit. In previous studies in mice with intracranial tumors, trastuzumab was reported to have no significant effect on survival at doses between 4 and 10 mg/kg, administered either daily or twice weekly (15, 16, 47). In our study, we did observe a slight increase in survival with unconjugated anti-HER2, but the effect was significantly smaller than that observed with ANG4043.

This demonstration of dose-dependent efficacy encourages further development of ANG4043 as an investigational agent indicated for human breast cancer brain metastases, a common end stage of breast cancer that is characterized by a particularly poor prognosis. Interestingly, increased survival with trastuzumab treatment has been reported in studies conducted in patients who have had whole brain radiotherapy (WBR) for breast cancer brain metastases (48). Overall survival for WBR-treated breast cancer patients with brain metastasis was 21 months for trastuzumab treated, compared with 9 months for chemotherapy treated and 3 months without treatment. The effects reported may be the result

Published OnlineFirst December 9, 2014; DOI: 10.1158/1535-7163.MCT-14-0399

of some degree of brain trastuzumab exposure, as WBR is believed to compromise the BBB. The CSF:plasma ratio of trastuzumab in patients with breast cancer is reported to increase 5- to 6-fold after WBR (49). Conjugation of our mAb with An2 increases brain mAb concentrations with the BBB intact, and therefore has potential for efficacy even in patients who have not received WBR.

Even for tumors outside of the brain, anti-HER2 treatment alone is insufficient to completely eradicate the disease. In the clinic, trastuzumab is coadministered with a cytotoxic anticancer therapeutic such as paclitaxel. Similar to the case for peripheral disease, treatment of metastatic breast cancer in the brain with mAb therapy will probably require coadministration with a brain-penetrant cytotoxic agent to achieve optimal response. Paclitaxel is commonly administered as an early-line therapy in breast cancer, but this small-molecule agent has shown little to no effect on brain metastases due to its poor penetration of the BBB (50). ANG1005 has been shown to cross the BBB efficiently. As this molecule has been shown to have promising antitumor activity in patients (28, 29), it is of significant interest to ascertain whether ANG4043 in combination with ANG1005 might have synergistic effects on breast cancer xenografts in preclinical models. Beyond coadministration, the next generation anti-HER2 therapy is adotrastuzumab emtansine, an antibody–drug conjugate (ADC) in which a highly potent cytotoxic maytansinoid drug is conjugated to trastuzumab and thereby targets HER2-positive tumor cells specifically (51). The An2 conjugation strategy is applicable to ADCs and is currently under investigation in our laboratory.

The An2 conjugation methodology described here can be applied to mAbs beyond anti-HER2 as well as to other classes of therapeutic proteins. Numerous tumor-targeting mAbs are in clinical use or clinical development, many of these for tumors that metastasize to brain. The preclinical efficacy of ANG4043 not only demonstrates that a treatment for HER2-positive brain metastasis is possible, but also offers a strategy for creation of brain-penetrant mAbs for a variety of brain tumors and other CNS disease.

Disclosure of Potential Conflicts of Interest

No potential conflicts of interest were disclosed.

Authors' Contributions

Conception and design: A. Regina, M. Demeule, S. Tripathy, J.-C. Currie, J.-P. Castaigne, J.E. Lachowicz

Development of methodology: A. Regina, M. Demeule, S. Tripathy, S. Lord-Dufour, J.-C. Currie, M. Iddir

Acquisition of data (provided animals, acquired and managed patients, provided facilities, etc.): A. Regina, S. Lord-Dufour, J.-C. Currie, M. Iddir, B. Annabi

Analysis and interpretation of data (e.g., statistical analysis, biostatistics, computational analysis): A. Regina, M. Demeule, S. Tripathy, S. Lord-Dufour, J.-C. Currie, M. Iddir, B. Annabi, J.E. Lachowicz

Writing, review, and/or revision of the manuscript: A. Regina, M. Demeule, S. Lord-Dufour, J.-C. Currie, J.-P. Castaigne, J.E. Lachowicz

Administrative, technical, or material support (i.e., reporting or organizing data, constructing databases): A. Regina

Study supervision: A. Regina, M. Demeule, B. Annabi

Acknowledgments

The authors thank Dr. John Lambert for helpful comments and Dr. David Norris, Ecosse Medical Communications, for editorial assistance.

Grant Support

This work was funded in part by a Collaborative Research and Development (CRD) grant from the Natural Sciences and Engineering Research Council of Canada (NSERC; RDCPJ 445033-12; to B. Annabi).

The costs of publication of this article were defrayed in part by the payment of page charges. This article must therefore be hereby marked *advertisement* in accordance with 18 U.S.C. Section 1734 solely to indicate this fact.

Received May 12, 2014; revised October 28, 2014; accepted October 29, 2014; published OnlineFirst December 9, 2014.

References

1. Jemal A, Bray F, Center MM, Ferlay J, Ward E, Forman D. Global cancer statistics. CA Cancer J Clin 2011;61:69–90.
2. Gonzalez-Angulo AM, Litton JK, Broglio KR, Meric-Bernstam F, Rakkhit R, Cardoso F, et al. High risk of recurrence for patients with breast cancer who have human epidermal growth factor receptor 2-positive, node-negative tumors 1 cm or smaller. J Clin Oncol 2009;27:5700–6.
3. Slamon DJ, Clark GM, Wong SG, Levin WJ, Ullrich A, McGuire WL. Human breast cancer: correlation of relapse and survival with amplification of the HER-2/neu oncogene. Science 1987;235:177–82.
4. Pegram MD, Lipton A, Hayes DF, Weber BL, Baselga JM, Tripathy D, et al. Phase II study of receptor-enhanced chemosensitivity using recombinant humanized anti-p185HER2/neu monoclonal antibody plus cisplatin in patients with HER2/neu-overexpressing metastatic breast cancer refractory to chemotherapy treatment. J Clin Oncol 1998;16:2659–71.
5. Shepard HM, Jin P, Slamon DJ, Pirot Z, Maneval DC. Herceptin. Handb Exp Pharmacol 2008:183–219.
6. Yin W, Jiang Y, Shen Z, Shao Z, Lu J. Trastuzumab in the adjuvant treatment of HER2-positive early breast cancer patients: a meta-analysis of published randomized controlled trials. PLoS ONE 2011;6:e21030.
7. Duchnowska R, Szczylik C. Central nervous system metastases in breast cancer patients administered trastuzumab. Cancer Treat Rev 2005;31:312–8.
8. Fuchs IB, Loebbecke M, Buhler H, Stoltenburg-Didinger G, Heine B, Lichtenegger W, et al. HER2 in brain metastases: issues of concordance, survival, and treatment. J Clin Oncol 2002;20:4130–3.
9. Wang W, Wang EQ, Balthasar JP. Monoclonal antibody pharmacokinetics and pharmacodynamics. Clin Pharmacol Ther 2008;84:548–58.
10. Lin YS, Nguyen C, Mendoza JL, Escandon E, Fei D, Meng YG, et al. Preclinical pharmacokinetics, interspecies scaling, and tissue distribution of a humanized monoclonal antibody against vascular endothelial growth factor. J Pharmacol Exp Ther 1999;288:371–8.
11. Gatson NN, Chiocca EA, Kaur B. Anti-angiogenic gene therapy in the treatment of malignant gliomas. Neurosci Lett 2012;527:62–70.
12. Kinoshita M, McDannold N, Jolesz FA, Hynynen K. Noninvasive localized delivery of Herceptin to the mouse brain by MRI-guided focused ultrasound-induced blood-brain barrier disruption. Proc Natl Acad Sci U S A 2006;103:11719–23.
13. Li Q, Shu Y. Pharmacological modulation of cytotoxicity and cellular uptake of anti-cancer drugs by PDE5 inhibitors in lung cancer cells. Pharm Res 2014;31:86–96.
14. Shin BJ, Burkhardt JK, Riina HA, Boockvar JA. Superselective intra-arterial cerebral infusion of novel agents after blood-brain disruption for the treatment of recurrent glioblastoma multiforme: a technical case series. Neurosurg Clin N Am 2012;23:323–9, ix-x.
15. Hu J, Ljubimova JY, Inoue S, Konda B, Patil R, Ding H, et al. Phosphodiesterase type 5 inhibitors increase Herceptin transport and treatment efficacy in mouse metastatic brain tumor models. PLoS ONE 2010;5:e10108.
16. Ningaraj NS, Sankpal UT, Khaitan D, Meister EA, Vats TS. Modulation of KCa channels increases anticancer drug delivery to brain tumors

Published OnlineFirst December 9, 2014; DOI: 10.1158/1535-7163.MCT-14-0399

and prolongs survival in xenograft model. Cancer Biol Ther 2009; 8:1924–33.
17. Boado RJ, Hui EK, Lu JZ, Sumbria RK, Pardridge WM. Blood–brain barrier molecular trojan horse enables imaging of brain uptake of radioiodinated recombinant protein in the rhesus monkey. Bioconjug Chem 2013;24: 1741–9.
18. Yu YJ, Zhang Y, Kenrick M, Hoyte K, Luk W, Lu Y, et al. Boosting brain uptake of a therapeutic antibody by reducing its affinity for a transcytosis target. Sci Transl Med 2011;3:84ra44.
19. Niewoehner J, Bohrmann B, Collin L, Urich E, Sade H, Maier P, et al. Increased brain penetration and potency of a therapeutic antibody using a monovalent molecular shuttle. Neuron 2014;81:49–60.
20. Pflanzner T, Janko MC, Andre-Dohmen B, Reuss S, Weggen S, Roebroek AJ, et al. LRP1 mediates bidirectional transcytosis of amyloid-beta across the blood-brain barrier. Neurobiol Aging 2011;32:2323 e1–11.
21. Uchida Y, Ohtsuki S, Katsukura Y, Ikeda C, Suzuki T, Kamiie J, et al. Quantitative targeted absolute proteomics of human blood-brain barrier transporters and receptors. J Neurochem 2011;117:333–45.
22. Zlokovic BV, Deane R, Sagare AP, Bell RD, Winkler EA. Low-density lipoprotein receptor-related protein-1: a serial clearance homeostatic mechanism controlling Alzheimer's amyloid beta-peptide elimination from the brain. J Neurochem 2010;115:1077–89.
23. Demeule M, Currie JC, Bertrand Y, Che C, Nguyen T, Regina A, et al. Involvement of the low-density lipoprotein receptor-related protein in the transcytosis of the brain delivery vector angiopep-2. J Neurochem 2008; 106:1534–44.
24. Demeule M, Regina A, Che C, Poirier J, Nguyen T, Gabathuler R, et al. Identification and design of peptides as a new drug delivery system for the brain. J Pharmacol Exp Ther 2008;324:1064–72.
25. Che C, Yang G, Thiot C, Lacoste MC, Currie JC, Demeule M, et al. New Angiopep-modified doxorubicin (ANG1007) and etoposide (ANG1009) chemotherapeutics with increased brain penetration. J Med Chem 2010;53:2814–24.
26. Regina A, Demeule M, Che C, Lavallee I, Poirier J, Gabathuler R, et al. Antitumour activity of ANG1005, a conjugate between paclitaxel and the new brain delivery vector Angiopep-2. Br J Pharmacol 2008;155:185–97.
27. Bertrand Y, Currie JC, Poirier J, Demeule M, Abulrob A, Fatehi D, et al. Influence of glioma tumour microenvironment on the transport of ANG1005 via low-density lipoprotein receptor-related protein 1. Br J Cancer 2011;105:1697–707.
28. Drappatz J, Brenner A, Wong ET, Eichler A, Schiff D, Groves MD, et al. Phase I study of GRN1005 in recurrent malignant glioma. Clin Cancer Res 2013;19:1567–76.
29. Kurzrock R, Gabrail N, Chandhasin C, Moulder S, Smith C, Brenner A, et al. Safety, pharmacokinetics, and activity of GRN1005, a novel conjugate of angiopep-2, a peptide facilitating brain penetration, and paclitaxel, in patients with advanced solid tumors. Mol Cancer Ther 2012;11:308–16.
30. Dagenais C, Rousselle C, Pollack GM, Scherrmann JM. Development of an in situ mouse brain perfusion model and its application to mdr1a P-glycoprotein-deficient mice. J Cereb Blood Flow Metab 2000;20:381–6.
31. Triguero D, Buciak J, Pardridge WM. Capillary depletion method for quantification of blood-brain barrier transport of circulating peptides and plasma proteins. J Neurochem 1990;54:1882–8.
32. Neels JG, van Den Berg BM, Lookene A, Olivecrona G, Pannekoek H, van Zonneveld AJ. The second and fourth cluster of class A cysteine-rich repeats of the low density lipoprotein receptor-related protein share ligand-binding properties. J Biol Chem 1999;274:31305–11.
33. Takasato Y, Rapoport SI, Smith QR. An *in situ* brain perfusion technique to study cerebrovascular transport in the rat. Am J Physiol 1984;247: H484–93.
34. Dagenais C, Avdeef A, Tsinman O, Dudley A, Beliveau R. P-glycoprotein deficient mouse in situ blood-brain barrier permeability and its prediction using an in combo PAMPA model. Eur J Pharm Sci 2009;38:121–37.
35. Varatharajan L, Thomas SA. The transport of anti-HIV drugs across blood-CNS interfaces: summary of current knowledge and recommendations for further research. Antiviral Res 2009;82:A99–109.
36. Baselga J, Norton L, Albanell J, Kim YM, Mendelsohn J. Recombinant humanized anti-HER2 antibody (Herceptin) enhances the antitumor activity of paclitaxel and doxorubicin against HER2/neu overexpressing human breast cancer xenografts. Cancer Res 1998;58:2825–31.
37. Moulder SL, Yakes FM, Muthuswamy SK, Bianco R, Simpson JF, Arteaga CL. Epidermal growth factor receptor (HER1) tyrosine kinase inhibitor ZD1839 (Iressa) inhibits HER2/neu (erbB2)-overexpressing breast cancer cells *in vitro* and *in vivo*. Cancer Res 2001;61:8887–95.
38. Wang CX, Koay DC, Edwards A, Lu Z, Mor G, Ocal IT, et al. *In vitro* and *in vivo* effects of combination of Trastuzumab (Herceptin) and Tamoxifen in breast cancer. Breast Cancer Res Treat 2005;92:251–63.
39. Yang MX, Shenoy B, Disttler M, Patel R, McGrath M, Pechenov S, et al. Crystalline monoclonal antibodies for subcutaneous delivery. Proc Natl Acad Sci U S A 2003;100:6934–9.
40. Khalili P, Arakelian A, Chen G, Singh G, Rabbani SA. Effect of Herceptin on the development and progression of skeletal metastases in a xenograft model of human breast cancer. Oncogene 2005;24:6657–66.
41. Thomas FC, Taskar K, Rudraraju V, Goda S, Thorsheim HR, Gaasch JA, et al. Uptake of ANG1005, a novel paclitaxel derivative, through the blood-brain barrier into brain and experimental brain metastases of breast cancer. Pharm Res 2009;26:2486–94.
42. Demeule M, Beaudet N, Regina A, Besserer-Offroy E, Murza A, Tetreault P, et al. Conjugation of a brain-penetrant peptide with neurotensin provides antinociceptive properties. J Clin Invest 2014;124:1199–213.
43. Sun X, Pang Z, Ye H, Qiu B, Guo L, Li J, et al. Co-delivery of pEGFP-hTRAIL and paclitaxel to brain glioma mediated by an angiopep-conjugated liposome. Biomaterials 2012;33:916–24.
44. Xin H, Sha X, Jiang X, Zhang W, Chen L, Fang X. Anti-glioblastoma efficacy and safety of paclitaxel-loading Angiopep-conjugated dual targeting PEG-PCL nanoparticles. Biomaterials 2012;33:8167–76.
45. Shao K, Huang R, Li J, Han L, Ye L, Lou J, et al. Angiopep-2 modified PE-PEG based polymeric micelles for amphotericin B delivery targeted to the brain. J Control Release 2010;147:118–26.
46. Couch JA, Yu YJ, Zhang Y, Tarrant JM, Fuji RN, Meilandt WJ, et al. Addressing safety liabilities of TfR bispecific antibodies that cross the blood-brain barrier. Sci Transl Med 2013;5:183ra57, 1–12.
47. Kodack DP, Chung E, Yamashita H, Incio J, Duyverman AM, Song Y, et al. Combined targeting of HER2 and VEGFR2 for effective treatment of HER2-amplified breast cancer brain metastases. Proc Natl Acad Sci U S A 2012;109:E3119–27.
48. Bartsch R, Rottenfusser A, Wenzel C, Dieckmann K, Pluschnig U, Altorjai G, et al. Trastuzumab prolongs overall survival in patients with brain metastases from Her2 positive breast cancer. J Neurooncol 2007; 85:311–7.
49. Stemmler HJ, Schmitt M, Willems A, Bernhard H, Harbeck N, Heinemann V. Ratio of trastuzumab levels in serum and cerebrospinal fluid is altered in HER2-positive breast cancer patients with brain metastases and impairment of blood-brain barrier. Anti-Cancer Drugs 2007;18:23–8.
50. Eiseman JL, Eddington ND, Leslie J, MacAuley C, Sentz DL, Zuhowski M, et al. Plasma pharmacokinetics and tissue distribution of paclitaxel in CD2F1 mice. Cancer Chemother Pharmacol 1994;34:465–71.
51. Lewis Phillips GD, Li G, Dugger DL, Crocker LM, Parsons KL, Mai E, et al. Targeting HER2-positive breast cancer with trastuzumab-DM1, an antibody-cytotoxic drug conjugate. Cancer Res 2008;68:9280–90.

Published OnlineFirst December 9, 2014; DOI: 10.1158/1535-7163.MCT-14-0399

Molecular Cancer Therapeutics

ANG4043, a Novel Brain-Penetrant Peptide–mAb Conjugate, Is Efficacious against HER2-Positive Intracranial Tumors in Mice

Anthony Regina, Michel Demeule, Sasmita Tripathy, et al.

Mol Cancer Ther 2015;14:129-140. Published OnlineFirst December 9, 2014.